Available online at www.sciencedirect.com
SCIENCE DIRECT®
Methods 37 (2005) 26–36
METHODS
www.elsevier.com/locate/ymeth

Multi-analyte surface plasmon resonance biosensing

Jiří Homola *, Hana Vaisocherová, Jakub Dostálek, Marek Piliarik

Institute of Radio Engineering and Electronics, Academy of Sciences of the Czech Republic, Chaberská 57, 18251 Prague, Czech Republic

Accepted 1 May 2005

Abstract

Surface plasmon resonance (SPR) biosensors are affinity sensing devices exploiting a special mode of electromagnetic field—surface plasmon-polariton—to detect the binding of analyte molecules from a liquid sample to biomolecular recognition elements immobilized on the surface of the sensor. In this paper, we review advances of SPR biosensor technology towards detection systems for the simultaneous detection of multiple analytes (multi-analyte detection). In addition, we report application of a recently developed multichannel SPR sensor based on spectroscopy of surface plasmons and wavelength division multiplexing of sensing channels to multi-analyte detection.

Keywords: Surface plasmon resonance; Biosensor; Multi-analyte detection, Affinity biosensing

1. Introduction

In the last two decades, we have witnessed remarkable progress in the development of biosensors and their applications in the areas such as environmental monitoring, biotechnology, medical diagnostics, drug screening, food safety, and security. Various sensor technologies have been developed (e.g., electrochemical sensors [1], piezoelectric sensors [2], electrical impedance sensors [3], and optical sensors [4]) and applied to detection of chemical and biological analytes [5]. Optical sensors offer several important features—they exhibit high sensitivity, their performance is insensitive to electromagnetic interference, and they do not require electrical signal in a sensing area. Optical methods exploited in affinity biosensors include fluorescence spectroscopy [6], label-free methods such as interferometry [7], spectroscopy of guide modes of dielectric waveguides (grating coupler [8], resonant mirror [9]), and metallic waveguides (surface plasmon resonance [10,11]).

This paper focuses on surface plasmon resonance (SPR) biosensors technology, reviews fundamentals of SPR sensing, and discusses advances of this technology towards multi-analyte detection. A special attention is given to a recently developed multichannel SPR sensor combining the wavelength division multiplexing of serially ordered sensing channels with the conventional parallel channel architecture. Application of this multichannel SPR sensor for simultaneous detection of multiple analytes is described.

2. Principle of operation of SPR biosensors

An affinity optical biosensor consists of an optical transducer and a biological recognition element (BRE) which interacts with an analyte. The SPR transducer incorporates a thin metal film which supports a special mode of electromagnetic field—a surface plasmon-polariton (SPP)—sometimes referred as to a surface plasma wave. The SPP propagates along the surface of the metal film and the intensity of its electromagnetic

* Corresponding author.
E-mail address: homola@ure.cas.cz (J. Homola).

1046-2023/$ - see front matter © 2005 Elsevier Inc. All rights reserved.
doi:10.1016/j.ymeth.2005.05.003

field exponentially decays from the metal surface into the adjacent medium. The most commonly used metal is gold due to its chemical stability. A change in the refractive index due to the binding of analyte molecules to biomolecular recognition elements immobilized on the metal surface results in a change in the propagation constant of the SPP [11]. Surface plasmon resonance biosensors take advantage of this phenomenon and measure changes in the propagation constant of the SPP to determine changes in the amount of bound analyte and subsequently the concentration of analyte in a sample. Changes in the propagation constant of the SPP are determined by measuring one of the characteristics of the light wave that excites the SPP. On the basis of the characteristic of the light wave which is measured, SPR sensors are classified as sensors with angular, wavelength, intensity, phase, and polarization modulations [11].

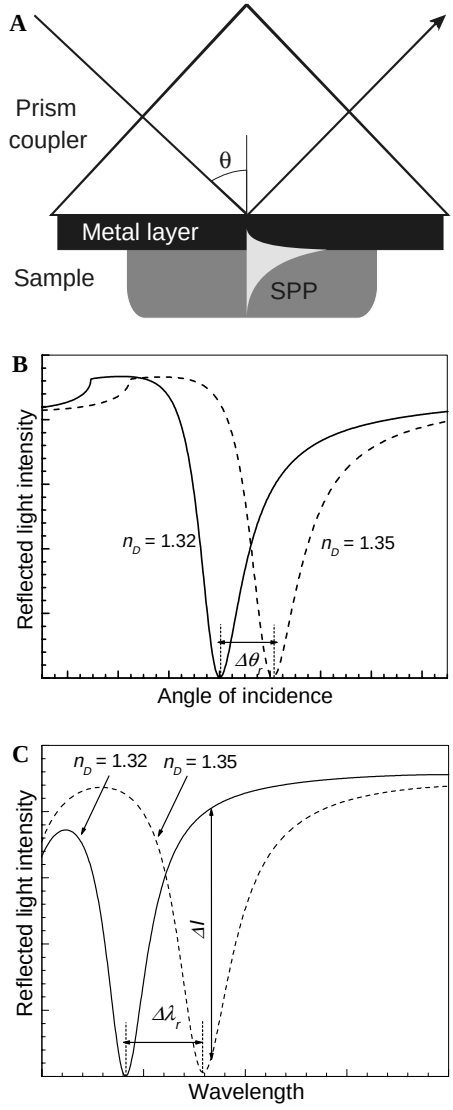

Fig. 1. (A) Excitation of surface plasmons via prism coupler. (B) Intensity of reflected light as a function of angle of incidence for a fixed wavelength and two refractive indices of sample. (C) Intensity of reflected light as a function of wavelength for a fixed angle of incidence and two refractive indices of sample.

The operating principle of the three modulation approaches (angular, wavelength, and intensity) used most frequently in SPR sensors is illustrated in Fig. 1, in which the excitation of surface plasmons is performed by the attenuated total reflection (ATR) in a prism coupler, Fig. 1A [11]. In SPR sensors with angular modulation, a beam of monochromatic light is used to excite an SPP (Fig. 1B). The propagation constant of the SPP and its changes are determined by measuring the intensity of reflected light at multiple angles of incidence and determining the angle of incidence yielding the strongest coupling with an SPP [12,13]. In SPR sensors with wavelength modulation, a beam of polychromatic light incident on the metal film under a fixed angle of incidence is used to excite an SPP (Fig. 1C). The propagation constant of the SPP and its changes are determined by measuring the intensity of reflected light at multiple wavelengths and determining the wavelength at which the strongest coupling with an SPP occurs [14]. In SPR sensors with intensity modulation, a beam of monochromatic light is made incident on the metal film under a fixed angle of incidence near the resonant angle of incidence (Fig. 1C) and changes in the intensity of reflected light are measured [15,16].

3. Advances in development of multi-analyte SPR sensors

3.1. Multichannel SPR sensor platforms

The most straightforward approach to multichannel SPR sensing is SPR imaging. SPR imaging is intensity modulation-based technique in which a collimated beam of monochromatic light passes through a prism coupler and excites SPPs on a thin metal layer. Intensity of the reflected light depends on the strength of the coupling between the light and SPPs which depends on the refractive index at the metal surface. Therefore, spatial distribution of the refractive index at the metal surface can be determined by measuring the distribution of light intensity across the reflected beam by means of a two-dimensional detector array (Fig. 2). This approach to spatially resolved SPR sensing has been applied to characterization of ultrathin films [17] and lipid layers [18,19].

When the metal surface is divided into multiple sensing spots, the SPR imaging device can be used as a multichannel SPR sensor. A multi-analyte biosensor based on SPR imaging was reported by Berger et al., [20], who demonstrated detection of four different analytes in a 16-channel matrix imaging format. SPR imaging was also applied to the observation of DNA hybridization [21], antibody–antigen binding, and

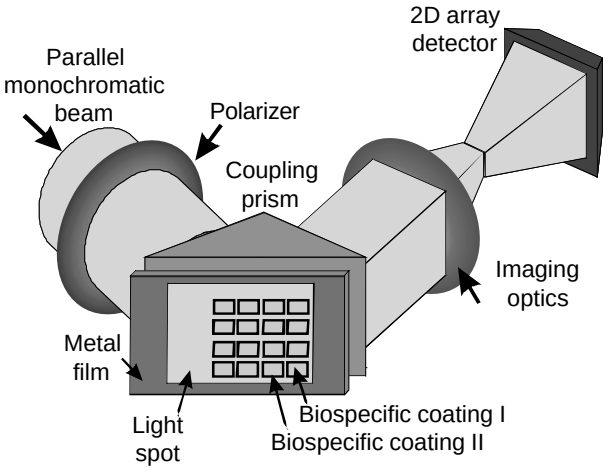

Fig. 2. SPR imaging sensor.

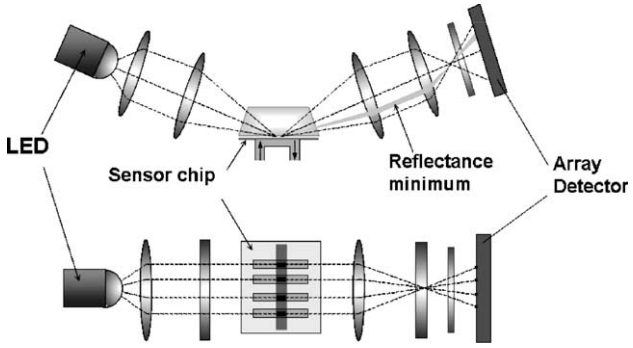

Fig. 3. SPR sensor with four parallel sensing channels (provided by S. Löfås, Biacore AB).

DNA–protein interaction [22], and detection of the sequence-specific binding of transcription regulatory proteins [23]. SPR imaging has also been exploited to study DNA-binding proteins to double-stranded DNA (dsDNA) array immobilized in a 10×12 array proving applicability of this method for monitoring the kinetics of binding of proteins to 120 different dsDNA sequences [24]. The major challenge for application of SPR imaging approach for biosensing is its rather limited resolution. Existing SPR imaging systems are capable of resolving bulk refractive index changes of about $\sim 10^{-5}$ RIU (refractive index units) [25]. To improve resolution of SPR imaging, this method was combined with polarization contrast and a spatially patterned multilayer SPR structure [26]. This approach generates high-contrast SPR images suitable for automated computer analysis, minimizes crosstalk between neighboring sensing channels, and provides compensation for light fluctuations improving the refractive index resolution to 3×10^{-6} RIU. This system was demonstrated to allow simultaneous monitoring of over 100 immunoreactions [26].

In contrast with SPR imaging systems, SPR sensors based on spectroscopy of surface plasmons take advantage of information contained in the whole wavelength or angular spectrum of light and therefore offer a considerably better resolution (up to 3×10^{-7} RIU) [27]. For multiplexing of sensing channels, most SPP spectroscopy-based sensors rely on parallel arrangement of sensing channels in which multiple light beams excite SPPs in different sensing channels and their reflectivity spectra are interrogated independently to determine SPR changes in each channel. Recently, SPR sensors based on serial channel architecture have also been reported. In these sensors, SPR spectra from multiple channels are encoded into a single optical wave [28,29]. Multichannel SPR sensors based on spectroscopy of SPP rely on ATR prism couplers [28–35] and diffraction gratings [36–38]. In ATR-based SPR biosensors with angular modulation and parallel architecture, series of convergent monochromatic beams are focused on a row of sensing channels where they excite SPPs. Light beams reflected from a row of sensing channels are projected on a two-dimensional detector array, Fig. 3. The first multi-channel SPR biosensors with angular modulation of SPR allowed simultaneous measurements in up to four sensing channels [30]; recently, the number of channels was extended to 6 [31], and 10 [32].

Lately, an interesting multichannel SPR sensor with angular interrogation and parallel sensing channels using a special planar sensor chip with diffractive optic coupling elements has been proposed. These elements project monochromatic light on an array of sensing channels and image the angular reflectivity spectra from each sensing channel on a CCD detector array [33]. In ATR-based SPR sensors with wavelength modulation and parallel architecture, series of collimated polychromatic beams are made incident on a row of sensing channels. SPR spectra encoded into the reflected light beams are analyzed by a spectrograph. The spectral analysis of multiple light beams is performed by multiple spectrographs [34] or by using an optical switch routing light from multiple channels to a spectrograph [35]. An alternative approach to multichannel SPR sensing with wavelength modulation is the wavelength division multiplexing (WDM). In the WDMSPR sensors, SPR spectra from multiple channels are encoded in different wavelength regions of a single polychromatic light beam. This is accomplished by changing the angle of incidence of the incident light beam (Fig. 4A) or by a dielectric overlayer deposited over a part of the SPR-active surface (Fig. 4B).

Multichannel sensors based on SPP spectroscopy have been also realized using diffraction grating couplers. These include an SPR compact disk platform employing a rotating sensor chip [36] and an HTS Biosystems SPR sensor in which SPR signal for each channel is determined from an angular reflectivity spectrum acquired by sequential angular scanning of SPR images

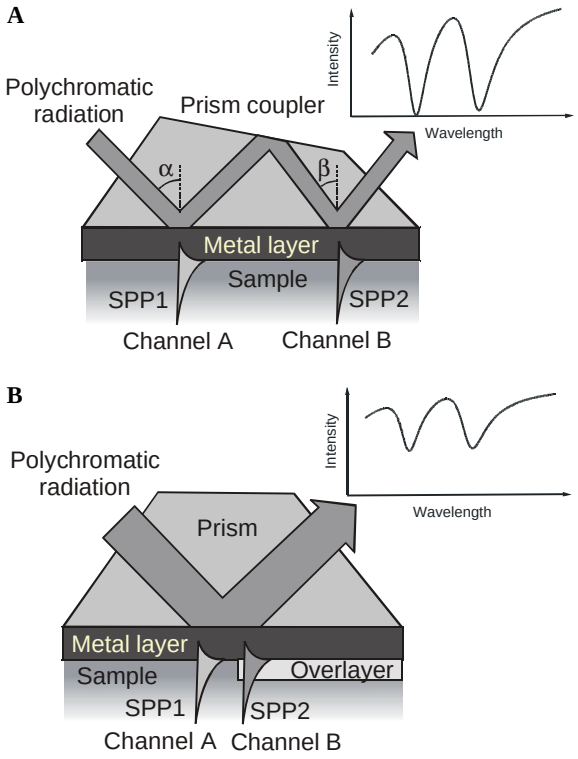

Fig. 4. SPR dual-channel sensors based on wavelength division multiplexing (WDM) of sensing channels. (A) WDM of sensing channels by means of altered angles of incidence [28]. (B) WDM of sensing channels by means of a high refractive index overlayer [29].

[37]. Another approach to multichannel SPR sensing is based on SPP spectroscopy on a two-dimensional array of diffraction gratings, where SPR angular spectra are sequentially scanned from rows of diffraction grating [38]. Mass production of diffraction grating-based SPR chips from plastics by technologies such as hot embossing or injection molding [39] offers potentially low-cost sensing elements [40] Fig. 5.

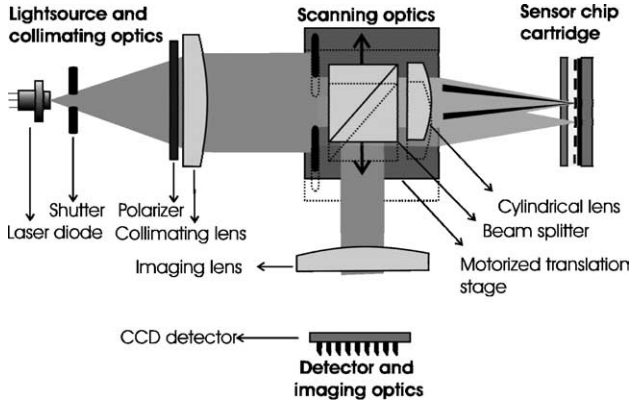

Fig. 5. Multi-channel SPR sensor based on an array of diffraction gratings [38].

3.2. Spatially controlled immobilization for multichannel SPR sensors

Various types of biomolecular recognition elements (antibodies [41], aptamers [42], peptides [43], and molecularly imprinted polymers [44], etc.) have been used in affinity biosensors. To enable multi-analyte detection, multiple biomolecular elements targeted to different analytes need to be immobilized in different sensing channels. This task requires the development of spatially controlled procedures for reproducible attachment of defined concentrations of biomolecular recognition elements on the surface of a sensor chip, Fig. 6. Other important requirements that these immobilization procedures have to fulfill are the conservation of biological activity of immobilized biomolecular recognition elements, non-fouling background of the sensor chip surface and the possibility to regenerate the biomolecular recognition elements (i.e., break their complex with the analyte molecules and make them available for another use).

In general, methods for immobilization of biomolecular recognition elements on gold films exploit physicochemical interactions such as chemisorptions [45], covalent binding [46,47], electrostatic coupling [48], and high-affinity molecular linkers in multilayer systems (e.g., streptavidin–biotin [49,50], proteins A or G [51], and complementary oligonucleotides [52]) and photo-immobilization (e.g., albumin derivatized with aryldiaziridines as a photo-linker [53]). One of the most remarkable techniques in surface chemistry is the spontaneous self-organization of *n*-alkylthiols or disulfides on gold into well-ordered arrays. Self-assembled monolayers (SAMs) have been employed in many immobilization methods for spatially controlled attachment of biomolecular recognition elements to surfaces of sensors [54]. To provide a desired surface concentration of biomolecular recognition elements on gold, mixed SAMs of long-chained ($n = 12$ and higher) *n*-alkylthiols terminated with functional group for further attachment of biomolecular recognition elements and short-chained alkylthiols for a non-fouling background have been developed [55,56].

To deliver molecular recognition elements to different areas of the SPR sensor surface, the immobilization chemistry needs to be spatially controlled. Most of the

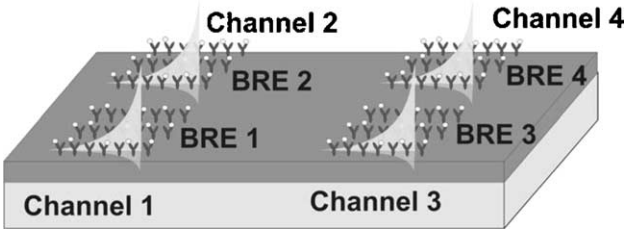

Fig. 6. Concept of multi-channel SPR biosensor.

current technologies of proteins arrays are based on the surfaces and formats that were earlier developed for DNA arrays. However, the chemical aspects of DNA array surfaces could not be easily adopted since proteins are chemically and structurally considerably more complex than nucleic acids and in contrast to DNA, they easily lose their biological activity due to denaturation, dehydration, or oxidation [57]. Most DNA array production techniques were developed for glass supports, but they can be tailored to noble metal surfaces with appropriate immobilization chemistries. Combination of SAMs with covalent coupling of biomolecular recognition elements or non-covalent streptavidin–biotin system as a linker for attachment of biotinylated biomolecular recognition elements are most frequently used approaches to development of protein arrays on gold.

Shumaker-Parry et al. [58] demonstrated microspotting double-stranded DNA on gold for SPR microscopy using two approaches. Both methods use streptavidin and biotinylated oligonucleotides. In the first method, the robotic microspotter was used to deliver nanoliter droplets of dsDNAs onto a uniform layer of streptavidin. In the second method, a streptavidin layer was also microspotted on a mixed-alkylthiol SAM and, subsequently, microspots of dsDNA were added using microspotting. Self-assembly surface chemistry and photopatterning have been combined to develop robust DNA and peptide arrays [59]. In the first step, a monolayer of 11-mercaptoundecylamine (MUAM) was assembled on gold surface. This amine-terminated surface was reacted with 9-fluorenylmethoxycarbonyl (Fmoc). Then, UV light was used to break the gold-thiol bonds and create bare gold pads, which were subsequently filled with MUAM. DNA or peptides were then attached to the MUAM using a covalent multi-step chemistry [59]. Finally, the Fmoc was removed and replaced with a polyethylene derivative to prevent non-specific binding. Another approach to the patterning of DNA or proteins on gold is based on microfluidic networks [60]. First, a set of parallel microchannels from poly(dimethylsiloxane) (PDMS) was created by replication of a silicon master prepared photolithographically. PDMS microchannels were used either to fabricate 1-D arrays consisting of lines of immobilized ligands or to create 2-D arrays in which a second set of PDMS microchannels was placed perpendicular to a 1-D line array. To create 1-D line arrays, the microchannels were attached to a gold surface modified with MUAM and activating reagents were introduced into the microchannels. Then, the DNA or peptides were reacted to the activated functional groups on MUAM. Subsequently, the microchannels were removed and the non-specific background was formed using polyethyleneglycol derivatives. Another approach is based on microcontact printing (μCP) which uses the relief pattern on the surface of an elastomeric PDMS stamp to form patterns on the sensor surface [61]. Various structures have been created on gold using μCP including patterned SAMs [62], proteins [63] or cells [64]. Peptide arrays have been formed using μCP onto reactive SAMs [65].

4. Multichannel SPR sensor with spectral modulation and wavelength division multiplexing

4.1. WDMSPR sensor

In this paper, we demonstrate multi-analyte detection using a recently developed eight-channel WDMSPR sensor [66]. This sensor is based on a special multireflection element in which a collimated beam of polychromatic light is made incident on the SPR sensor surface under two slightly different angles of incidence (Fig. 4A). Upon the first incidence on the surface of the sensor (channel A), light excites an SPP at the outer metal surface at the wavelength λ_A. The excitation of the SPPs produces a sharp absorption dip in the spectrum of optical wave centered at the wavelength λ_A. The reflected light is redirected inside the element and made incident on the metal film in the second region (channel B) under a different angle of incidence β ($\beta < \alpha$). At this angle of incidence, the optical wave couples to an SPP at a longer wavelength λ_B ($\lambda_B > \lambda_A$) generating a dip in the spectrum of the optical wave centered at the wavelength λ_B. Consequently, the wavelength spectrum of the transmitted light exhibits two SPR dips corresponding to SPRs in two distinct areas of the metal film, Fig. 7. These areas form two independent sensing channels. Response of each channel is encoded into a shift in the position of respective SPR dip.

The WDMSPR system reported herein combines the wavelength division multiplexing of pairs of sensing

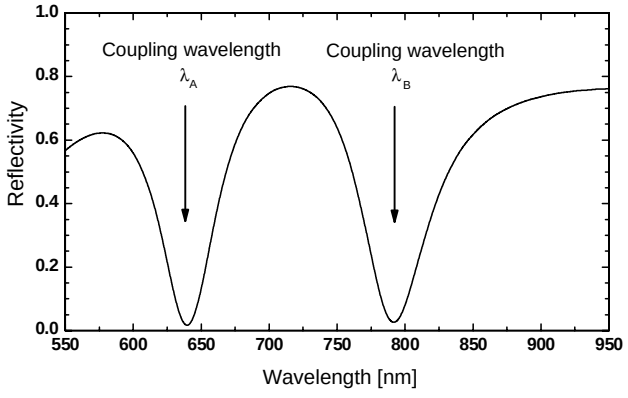

Fig. 7. Reflectivity in the WDMSPR sensing element as a function of wavelength. Sensing element—SF14 glass, metal layer–gold, thickness –55 nm, dielectric–aqueous medium, angles of incidence $\alpha = 54.6°$ and $\beta = 52.5°$.

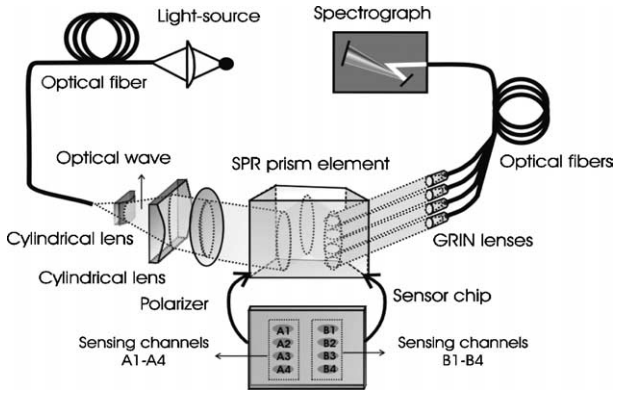

Fig. 8. An eight-channel SPR sensor combining parallel architecture with the wavelength division multiplexing of serially ordered channels.

channel with four parallel light beams to provide the total of eight sensing channels, Fig. 8. In the developed prototype of the sensor, polychromatic light from a halogen lamp (Avalight-Hal from Avantes, Netherlands) was coupled into an optical fiber (FT-400-EMT from Thorlabs, USA) and collimated using two cylindrical lenses. The collimated light beam was polarized by a dichroic polarizer (Polarcor, USA) and coupled in the WDMSPR sensing element to which a sensor chip (SF14 glass slide) coated by an adhesion promoting chromium layer (thickness less than 2 nm) and SPR-active gold layer (thickness 55 nm) was attached. The light was made incident on the SPR-active surface in eight areas denoted as A1–A4 and B1–B4, Fig. 8. Light beams reflected at the sensing areas A1–A4 and B1–B4 were collected by four miniature GRIN lenses (NSG America, USA) and coupled to four optical fibers FT-400-EMT (Thorlabs, USA) connected to a four-channel spectrograph S2000 (Ocean Optics, USA). The SPR spectra were measured in TM polarization and normalized with spectra obtained in TE polarization. Measured SPR spectra were averaged in time and the SPR dip position was determined by the 5th-order polynomial fitting and tracked over time for each sensing channel. An eight-channel flow-cell was clamped against the SPR chip to contain liquid samples during experiments. The flow-cell was made of an acrylic substrate with input and output ports interfacing flow-cell chambers for each sensing channel. The flow-cell chambers were cut into a gasket made of a 50-micrometer thick polyurethane sheet using a CO_2 laser beam (custom made by Micronics, USA). The volume of each flow-cell chamber was 2 μl. Input flow-cell ports were connected via tubings (Upchurch Scientific, USA) with two four-channel peristaltic pumps Reglo Digital (Ismatec, Switzerland) which controlled the flow of liquid samples through the flow-cell. In the reported experiments, the flow rate of 50 μl/min was used.

4.2. Materials

Antibody solutions were prepared in 10 mM phosphate buffer (PB), pH 7.6, at 20 °C. Analyte solutions were prepared in PBS (10 mM phosphate buffer, 137 mM NaCl, and 2.7 mM KCl, pH 7.4, at 20 °C) containing bovine serum albumin at a concentration of 100 μg/ml. Bovine serum albumin (BSA) was purchased from Sigma–Aldrich, USA. The C_{11}-chained and C_{16}-chained alkanethiols (C_{11}-mercapto-1-undecanol and C_{16}-mercaptohexadecanoic acid) and the *N*,*N*,*N*′,*N*′-tetramethyl-*O*-(*N*-succinimidyl)uronium tetrafluoroborate (TSTU) used for activation of carboxylic terminal groups on C_{16} alkanethiol were purchased from Sigma–Aldrich, USA. Monoclonal affinity-purified antibodies against human immunoglobulin E (aIgE), human immunoglobulin G (aIgG), human choriogonadotropin (ahCG), and horseradish peroxidase (aPx) were purchased from Seva Immuno, Czech Republic. Human immunoglobulin E (IgE) was purchased from Biodesign, USA, human immunoglobulin G (IgG) was obtained from the Faculty of Sciences of the Charles University (Laboratory of Anthropology and Human Genetics), Czech Republic, human choriogonadotropin (hCG) was purchased from Calbiochem, USA, and horseradish peroxidase (Px) from Kem-En-Tec, Denmark. Immune reaction activities of all immune partners were confirmed by ELISA method.

4.3. Chip functionalization

The functionalized method used in this work is based on thiol-attachment chemistry and spatially controlled delivery of antibodies using microfluidics. Prior to functionalization, sensor chips were rinsed with Piranha solution (a 1:3 mixture of 30% hydrogen peroxide and 96% sulfuric acid) for 3 min, then washed with deionized water and dried with nitrogen stream. A 7:3 mixture of

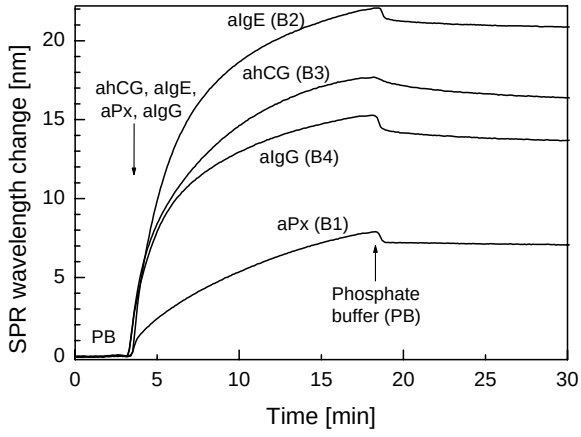

Fig. 9. SPR wavelength change due to the immobilization of aPx, aIgE, ahCG, and aIgG antibodies, antibody concentration—50 μg/ml.

C_{11}-chained and C_{16}-chained alkanethiols was dissolved in degassed absolute ethanol with a total thiol concentration of 1 mM. The C_{16} alkanethiols terminated with a carboxylic head group were used to anchor an antibody; C_{11} alkanethiol chains terminated with a hydroxyl head group were used to form a non-fouling background. Sensor chips were immersed in a thiol solution and stored in a dark place at room temperature for two days.

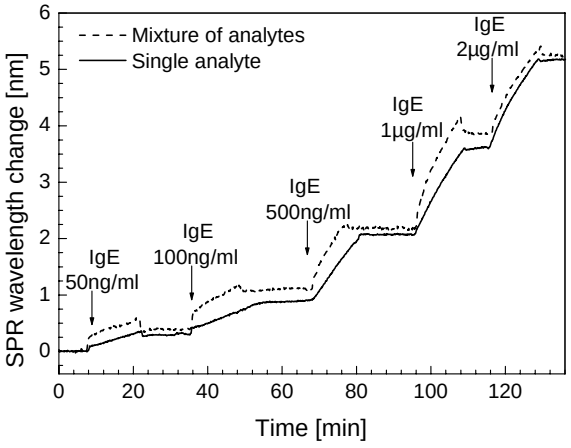

Fig. 10. IgE sensorgrams for solutions containing only IgE (channel B2) and the mixture of analytes (channel A2).

After the formation of a thiol self-assembled monolayer (SAM), the sensor chips were rinsed with ethanol, dried with nitrogen, rinsed with water, and dried with nitrogen again. The carboxylic terminal groups on the sensor surface were activated by TSTU dissolved in dimethylformamide at a concentration of 1 mg/ml for 4 h. After the activation, the sensor chip was rinsed with water, dried with nitrogen, and loaded into the SPR instrument. Antibody attachment was performed in situ by flowing phosphate buffer solution with 50 µg/ml of antibody along a sensing channel surface for 15 min (flow rate 50 µl/min). Specifically, identical solutions containing aPx, aIgE, ahCG, and aIgG were flowed through pairs of sensing channels A1 and B1, A2 and B2, A3 and B3, and A4 and B4, respectively. Then, the antibody solutions were replaced with a phosphate buffer solution containing natrium chloride at a concentration of 1 M, which was flowed through all channels to remove weakly bound antibodies. The immobilization of the aPx, aIgE, ahCG, and aIgG antibodies on the thiol-coated SPR sensing surface was observed using the SPR sensor system described in Section 4.1. Fig. 9 shows the sensor response to the immobilization of antibodies in the sensing channels B1–B4. The sensor response to antibodies ranges from 9 to 23 nm. This difference is believed to be mainly due to different accessibilities of amino groups

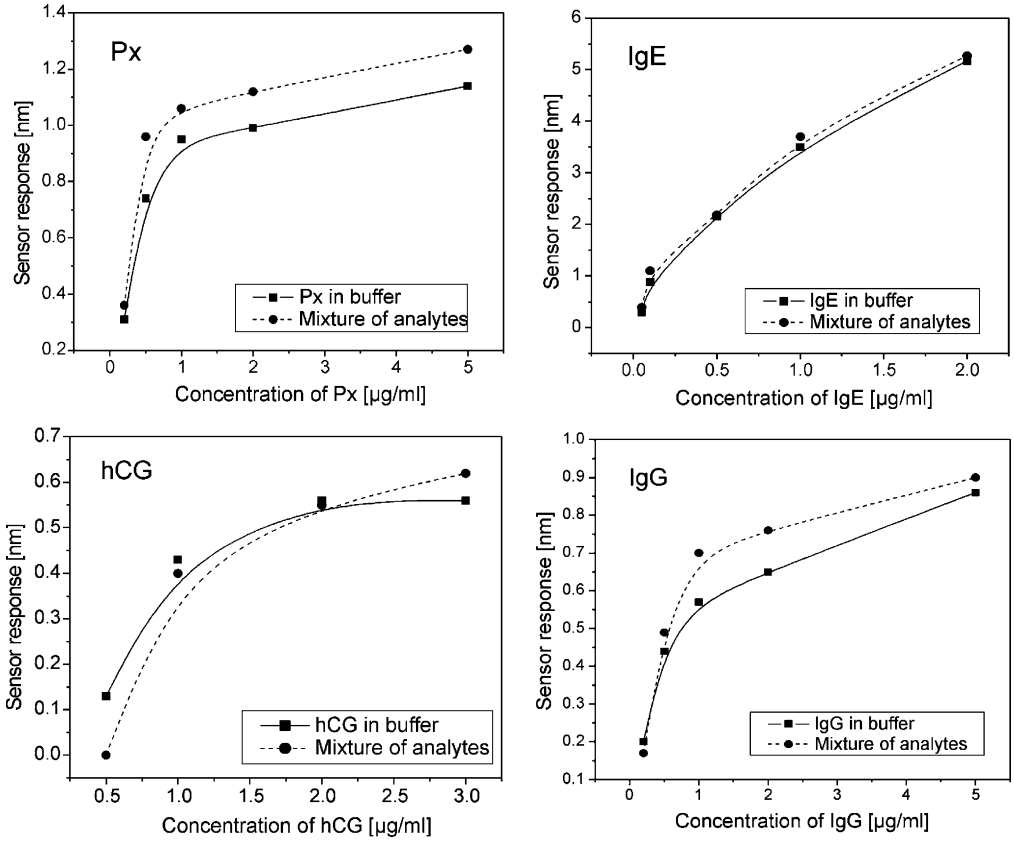

Fig. 11. Sensor response as a function of analyte concentration for Px, IgE, hCG, and IgG measured in pure buffer and mixture of all analytes.

for each type of antibody and electrostatic interaction between the antibody and the surface. Finally, the sensor surface was flushed with BSA dissolved in PBS to interact with the unreacted carboxylic groups.

4.4. Multi-analyte detection

The SPR chip coated with aPx, aIgE, ahCG, and aIgG antibodies was used for simultaneous detection of model analytes—Px, IgE, hCG, and IgG. Detection of these analytes was performed in solutions containing only a single analyte and in mixtures containing Px, IgE, hCG, and IgG. First, buffer (BSA-PBS) was flowed through all eight sensing channels until a stable sensor response was reached. Then, the mixture of Px, IgE, hCG, and IgG was flowed through the sensing channels A1–A4 for 15 min. Simultaneously, four solutions containing only the analyte corresponding to the immobilized antibody at the concentration identical to the one in the mixtures were injected into the sensing channels B1–B4. After the incubation for 15 min, these samples were replaced with buffer. This procedure was performed sequentially with solutions containing Px, hCG, IgG, and IgE at concentrations of 0.2, 0.5, 0.2, and 0.05 μg/ml (MIX 1); 0.5, 1, 0.5, and 0.1 μg/ml (MIX 2); 1, 2, 1, and 0.5 μg/ml (MIX 3); 2, 3, 2, and 1 μg/ml (MIX 4); and 5, 5, 5, and 2 μg/ml (MIX 5), respectively. Typical sensorgrams for samples containing only a single analyte and in mixtures of analytes are shown in Fig. 10.

The sensor response to an increasing concentration of pure analytes and analytes in mixtures was simultaneously measured. The sensor response was determined as a difference in the resonant wavelength in buffer before and after the incubation of the sensor surface with samples. The resulting sensor responses as a function of concentration of analyte are shown in Fig. 11. The reproducibility of the measurements was evaluated in repeated experiments and found to be within ± 10% of the sensor response for Px, hCG, and IgG and ± 5% of the sensor response for IgE. The difference in the sensor response to the same concentration of target analyte in the absence and in the presence of other analytes was found to fall within 18%. Moreover, it was observed that the sensor response to analyte in a mixture was usually higher than that corresponding to a pure sample containing only analyte.

To investigate the specificity of studied biomolecular interactions, the sensor responses to non-target and target analytes were compared. The non-target analytes followed with the target analyte were sequentially flowed

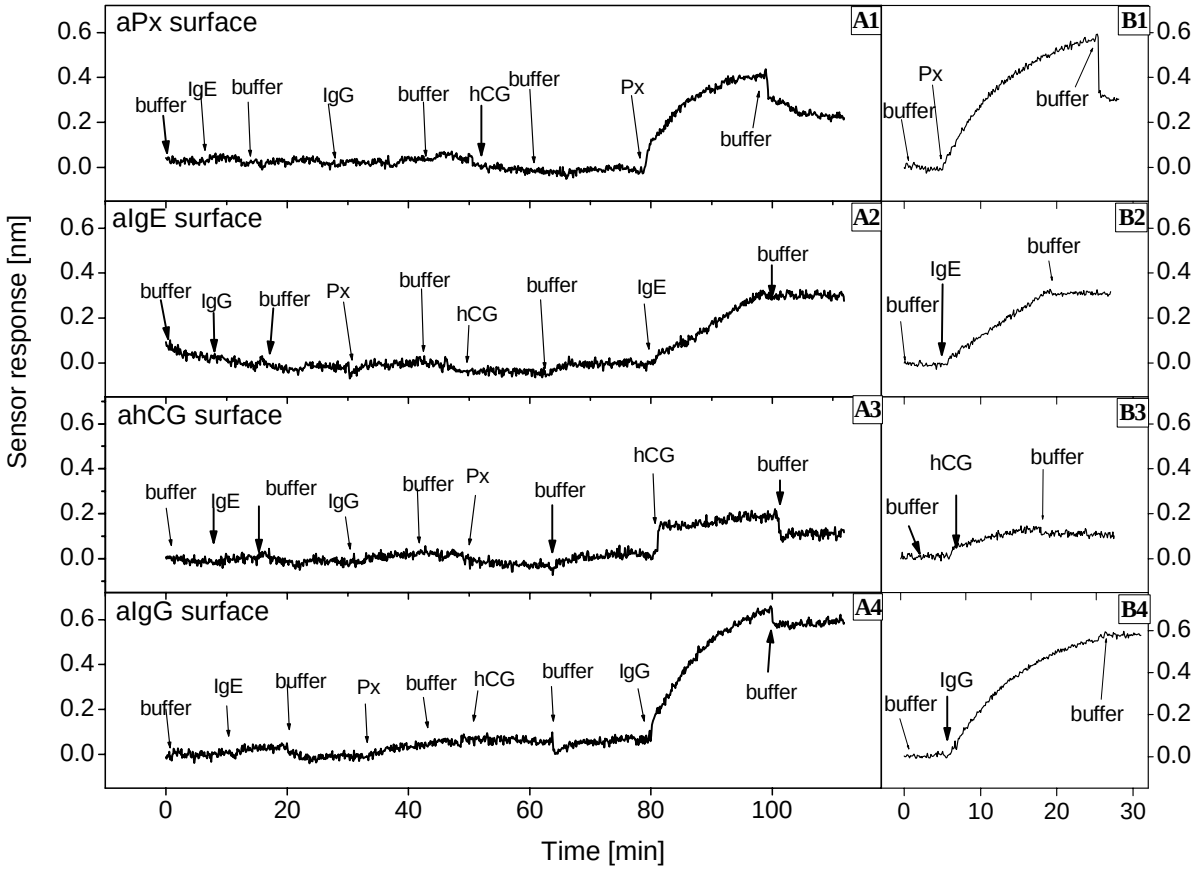

Fig. 12. Sensor response to target analytes injected after a sequence of non-target analytes (A1–A4) and sensor response to specific analytes without the exposure to non-target analytes (channels B1–B4), concentrations of Px, IgE, hCG, and IgG are 0.5, 0.1, 0.5, and 0.5 μg/ml, respectively.

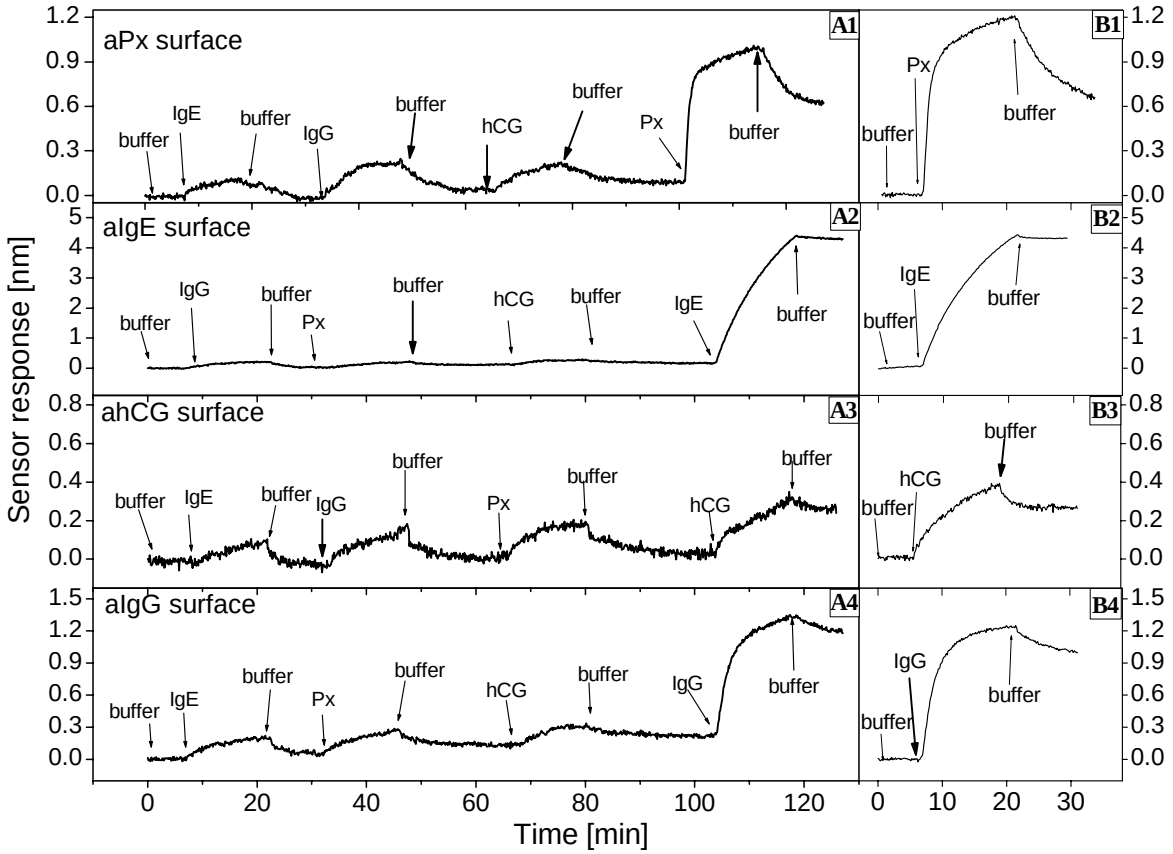

Fig. 13. Sensor response to a target analyte injected after a sequence of non-target analytes (A1–A4) and directly (channels B1–B4), concentrations of Px, IgE, hCG, and IgG are 5, 2, 2, and 5 μg/ml, respectively.

through the sensing channels A1–A4. Simultaneously, solutions with only a specific analyte were flowed through the sensing channels B1–B4. The same experiment was performed for lower and higher concentrations of analyte molecules. Corresponding sensorgrams for low and high concentrations are shown in Figs. 12 and 13, respectively. Concentrations of Px, IgE, hCG and IgG were 0.5, 0.1, 0.5, and 0.5 μg/ml, and 5, 2, 2, and 5 μg/ml for low and high concentrations, respectively.

As follows from Fig. 12, the low concentrations of non-target analytes generated basically no response (less than 0.07 nm) and the subsequent response to the target analytes produced sensor response of 0.25, 0.30, 0.10, and 0.54 nm for Px, IgE, hCG, and IgG, respectively. These values agree well with the sensor responses to samples containing only a target analyte observed in the sensing channels not in contact with the non-target analytes, which were found to be 0.30, 0.30, 0.10, and 0.56 nm for Px, IgE, hCG, and IgG, respectively. High analyte concentrations produced non-specific sensor responses of about 0.1, 0.17, 0.03, and 0.22 nm, on aPx, aIgE, ahCG, and aIgG-coated surfaces, respectively. The subsequent binding of the target analyte produced sensor responses of about 0.62, 4.10, 0.24, and 1.00 nm for Px, IgE, hCG, and IgG, respectively. As follows from the experimental data, majority of the non-specific binding was reversible (Fig. 13) and the observed non-specific response was about 16, 3, 13, and 22% of the specific response to Px, IgE, hCG, and IgG, respectively. Responses to the same concentrations of pure analytes incubated with sensing surfaces unexposed to other analytes were found to be 0.65, 4.3, 0.27, and 1.01 nm for Px, IgE, hCG, and IgG, respectively; Fig. 13.

The ultimate lowest detection limits of the sensor for the model analytes were estimated based on the accuracy of measuring the SPR wavelength that is defined as three standard deviations of sensor response noise and was equal to 0.03 nm for the used WDMSPR sensor system. In pure samples, the ultimate detection limits were 60, 10, 150, and 30 ng/ml for Px, IgE, hCG, and IgG, respectively. Detection of low concentrations of analytes in mixtures was limited by the non-specific binding and determined to be 200, 600, 300, and 200 ng/ml, Px, IgE, hCG, and IgG, respectively.

5. Outlook

A number of surface plasmon resonance (SPR) sensor platforms and attachment/patterning methods suitable

for multi-analyte detection have been proposed over the last decade. So far, the majority of demonstrated SPR multi-sensors have been able to detect simultaneously only a limited number of analytes. However, further advances in development of biomolecular recognition element arrays and microfluidics for both patterning and sample distribution are expected to lead to SPR systems capable of observing and quantifying tens and hundreds of biomolecular interactions in near future. Implementations of such multi-analyte sensors will be driven by the needs of specific applications. The main application areas include pharmaceutical research (high-throughput systems for drug screening), medical diagnostics (high-throughput diagnostic tools), food safety (systems for rapid detection of foodborne pathogens and agents), and security (devices for early detection and identification of biological and chemical warfare agents).

Acknowledgments

The authors thank Václav Malina and Petra Chocholáčová (Institute of Radio Engineering and Electronics, Prague) for deposition of thin films, Jiří Škvor (Seva Immuno, Ltd., Prague) for providing antibodies used in this work, and Markéta Lachmanová for assistance with experiments. This work was supported by the Grant Agency of the Czech Republic under contracts 303/03/0249, 203/02/1326, 102/03/0633, and 202/05/0628 and by European Commission under contract QLK4-CT-2002-02323.

References

[1] A.L. Ghindilis, P. Atanasov, M. Wilkins, E. Wilkins, Biosens. Bioelectron. 13 (1998) 113–131.
[2] X. Chu, Z.H. Lin, G.L. Shen, R.Q. Yu, M. Analyst. 120 (1995) 2829–2832.
[3] P. Pless, K. Futschik, E. Schopf, J. Food Prot. 57 (1994) 369–376.
[4] G. Gauglitz G, Sensor Update Vol. 1, VCH Verlagsgesellschaft, Weinheim 1996.
[5] D. Ivnitski, I. Abdel-Hamid, P. Atanasov, E. Wilkins, Biosens. Bioelectron. 14 (1999) 599–624.
[6] C.A. Rowe-Taitt, J.W. Hazzard, K.E. Hoffman, J.J. Cras, J.P. Golden, F.S. Ligler, Biosens. Bioelectron. 15 (2000) 579–589.
[7] R.G. Heideman, R.P.H. Kooyman, J. Greve, Sens. Act. B 10 (1993) 209–217.
[8] D. Clerc, W. Lukosz, Sens. Act. B 19 (1994) 581–586.
[9] R. Cush, J.M. Cronin, W.J. Stewart, C.H. Maule, J. Molloy, N.J. Goddard, Biosens. Bioelectron. 8 (1993) 347–353.
[10] J. Homola, S. Yee, G. Gauglitz, Sens. Act. B 54 (1999) 3–15.
[11] J. Homola, S.S. Yee, D. Myszka, Surface plasmon biosensors, in: F.S. Ligler (Ed.), Optical Biosensors: Present and Future, Elsevier, Amsterdam, 2002.
[12] K. Matsubara, S. Kawata, S. Minami, Appl. Opt. 27 (1988) 1160–1163.
[13] B. Liedberg, I. Lundstrom, E. Stenberg, Sens. Act. B 11 (1993) 63–72.
[14] L.M. Zhang, D. Uttamchandani, Electron. Lett. 23 (1988) 1469–1470.
[15] C. Nylander, B. Liedberg, T. Lind, Sens. Act. 3 (1982) 79–88.
[16] M.M.B. Vidal, R. Lopez, S. Aleggret, J. Alonso-Chamarro, I. Garces, J. Mateo, Sens. Act. B 11 (1993) 455–459.
[17] B. Rothenhäusler, W. Knoll, Nature 332 (1988) 615–617.
[18] W. Hickel, W. Knoll, Thin Solid Films 187 (1990) 349–356.
[19] R.P.H. Kooyman, U.J. Krull, Langmuir 7 (1991) 1506–1509.
[20] C.E.H. Berger, T.A.M. Beumer, R.P.H. Kooyman, J. Greve, Anal. Chem. 70 (1998) 703–706.
[21] A.J. Thiel, A.G. Frutos, C.E. Jordan, R.M. Corn, L.M. Smith, Anal. Chem. 69 (1997) 4948–4956.
[22] G.J. Wegner, H.L. Lee, G. Marriott, R.M. Corn, Anal. Chem. 75 (2003) 4740–4746.
[23] E.A. Smith, M.G. Erickson, A.T. Ulijasz, B. Weisblum, R.M. Corn, Langmuir 19 (2003) 1486–1492.
[24] J.S. Shumaker-Parry, R. Aebersold, C.T. Campbell, Anal. Chem. 76 (2004) 2071–2082.
[25] E. Fu, T.M. Chinowsky, J. Foley, J. Weinstein, P. Yager, Rev. Sci. Instrum. 75 (2004) 2300–2304.
[26] M. Piliarik, H. Vaisocherová, J. Homola, Biosens. Bioelectron. 20 (2005) 2104–2110.
[27] R. Karlsson, R. Stahlberg, Anal. Biochem. 228 (1995) 280–284.
[28] J. Homola, J. Dostálek, J. Etyroký, Proc. SPIE 4416 (2001) 86–89.
[29] J. Homola, H.B. Lu, G.G. Nenninger, J. Dostálek, S.S. Yee, Sens. Act. B 76 (2001) 403–410.
[30] S. Löfas, M. Malmqvist, I. Rönnberg, E. Stenberg, B. Liedberg, I. Kundström, Sens. Act. B 5 (1991) 79–84.
[31] R. Karlsson, J. Mol. Recogn. 17 (2004) 151–161.
[32] M.J. O'Brien, V.H. Perez-Luna, S.R.J. Brueck, G.P. Lopez, Biosens. Bioelectron. 16 (2001) 97–108.
[33] C. Thirstrup, W. Zong, M. Borre, H. Neff, H.C. Pedersen, G. Holzhueter, Sens. Act. B 100 (2004) 298–308.
[34] J. Homola, J. Dostálek, S.F. Chen, A. Rasooly, S. Jiang, S.S. Yee, Int. J. Food Microbiol. 75 (2002) 61–69.
[35] G.G. Nenninger, J.B. Clendenning, C.E. Furlong, S.S. Yee, Sens. Act. B 51 (1998) 38–45.
[36] W.A. Challener, R.R. Ollman, K.K. Kam, Sens. Act. B 56 (1999) 254–258.
[37] J.M. Brockman, S.M. Fernandez, Am. Lab. 33 (2001) 37–40.
[38] J. Dostálek, J. Homola, M. Miler, Sens. Act. B 108 (2005) 758–764.
[39] M.T. Gale, Microelectron. Eng. 34 (1997) 321–339.
[40] C.R. Lawrence, N.J. Geddes, D.N. Furlong, J.R. Sambles, Biosens. Bioelectron. 11 (1996) 389–400.
[41] B. Hock, Anal. Chem. Acta 347 (1997) 177–186.
[42] S.D. Jayasena, Clin. Chem. 45 (1999) 1628–1650.
[43] G.J. Wegner, H.J. Lee, G.M. Corn, Anal. Chem. 74 (2002) 5161–5168.
[44] R.J. Ansell, O. Ramstrom, K. Mosbach, Clin. Chem. 42 (1996) 1506–1512.
[45] R.C. Nuzzo, D.L. Allaza, J. Am. Chem. Soc. 105 (1983) 4481–4483.
[46] B. Johnsson, S. Lofas, G. Lindquirst, A. Edstrom, R.M. Muller Hillgren, A. Hansson, J. Mol. Recog. 8 (1995) 125–131.
[47] D.J. O'Shanneessy, M. Brigham-Burke, K. Peck, Anal. Biochem. 314 (2001) 1–26.
[48] M. Houska, E. Brynda, K. Bohatá, J. Colloid Interf. Sci. 273 (2004) 140–147.
[49] S. Tombelli, M. Mascini, A.P.F. Turner, Biosens. Bioelectron. 17 (2002) 929–936.
[50] S. Busse, E. Scheumann, B. Menges, S. Mittler, Biosens. Bioelectron. 17 (2002) 704–710.
[51] G.P. Anderson, M.A. Jacoby, F.S. Ligler, K.D. King, Biosens. Bioelectron. 12 (1997) 329–336.
[52] J. Ladd, C. Boozer, Q. Yu, S. Chem, J. Homola, S. Jiang, Langmuir 20 (2004) 8090–8095.
[53] H. Gao, M. Sanger, R. Luginbuhl, H. Sigrist, Biosens. Bioelectron. 10 (1995) 317–328.
[54] W. Knoll, M. Liley, D. Piscevic, J. Spinke, M.J. Tarlov, Adv. Biophys. 34 (1997) 231–251.

[55] L.S. Jung, K.E. Nelson, P.S. Stayton, C.T. Campbell, Langmuir 16 (2000) 9421–9432.
[56] K.E. Nelson, L. Gamble, L.S. Jung, M.S. Boeckl, E. Neemi, S.L. Golledge, T. Sasaki, D.G. Castner, C.T. Campbell, P.S. Stayton, Langmuir 17 (2001) 2807–2816.
[57] M.K. Baller, L.R. Booth, J.F. Burke, R.M. Corn, G. Franklin, J. Fritz, K.A. Hughes, R.J. Kaiser, D. Kambhampati, W. Knoll, H.J. Lee, S. Lofas, in: D. Kambhampati (Ed.), Protein Microarray Technology, Wiley-VCH, Weinheim, 2004.
[58] J.S. Shumaker-Parry, M.H. Zareie, R. Aebersold, C.T. Campbell, Anal. Chem. 76 (2004) 918–929.
[59] J.M. Brockman, A.G. Frutos, R.M. Corn, J. Am. Chem. Soc. 121 (1999) 8044–8051.
[60] R.J. Jackman, D.C. Duffy, E. Ostuni, N.D. Willmore, G.M. Whitesides, Anal. Chem. 70 (1998) 2280–2287.
[61] J. Lahiri, E. Ostuni, G.M. Whitesides, Langmuir 15 (1999) 2053–2060.
[62] R.K. Smith, P.A. Lewis, P.S. Weiss, Progr. Surf. Sci. 75 (2004) 1–68.
[63] H.B. Lu, J. Homola, C.T. Campbell, G.G. Nenninger, S.S. Yee, B.D. Ratner, Sens. Act. B 74 (2001) 91–99.
[64] R.S. Kane, S. Takayama, E. Ostuni, D.E. Ingber, G.M. Whitesides, Biomaterials 20 (1999) 2363–2376.
[65] L. Yan, X-M. Zhao, G.M. Whitesides, J. Am. Chem. Soc. 120 (1998) 6179–6180.
[66] J. Dostálek, H. Vaisocherová, J. Homola, Sens. Act. B 107 (2005) 154–161.